the heat-transfer rate. The effect becomes less noticeable, however, as y increases.

The oncoming boundary-layer thickness δ is expressed indirectly by S^* and its main effect is found in its influence on the dividing streamline velocity U_d. For the case of constant external flow conditions, S^* is proportional to w/S_b. Also under these conditions δ is proportional to $S_b^{1/2}$. Thus, S^* is proportional to δ^{-2} and (if $S^* < 0.01$) U_d and $T_d - T_w$ are both proportional to $\delta^{-2/3}$. The net result is that the local heat-transfer rate is proportional to $\delta^{-4/3}$. That is, increases in the oncoming boundary-layer thickness will decrease the convective heat-transfer rate within the cavity.

References

[1] Hunt, L. R. and Howell, R. R., "Exploratory Study of Open-Face Honeycomb to Reduce Temperature of Hypersonic Aircraft Structure," TN D-5278, 1969, NASA.

[2] Wieting, A. R., "Experimental Investigation of Heat Transfer Distributions in Deep Cavities in Hypersonic Separated Flow," TN D-5908, 1970, NASA.

[3] Burggraf, O. R., "A Model of Steady Separated Flow in Rectangular Cavities at High Reynolds Number," *Proceedings of the 1965 Heat Transfer and Fluid Mechanics Institute*, 1965, Stanford University Press, Stanford, Calif. pp. 190–229.

[4] Nestler, D. E., "Laminar Heat Transfer to Cavities in Hypersonic Low Density Flow," *Proceedings of the Third International Heat Transfer Conference*, American Society of Mechanical Engineers, Vol. II, 1966, pp. 251–261.

[5] Chung, P. M. and Viegas, J. R., "Heat Transfer at the Reattachment Zone of Separated Laminar Boundary Layers," TN D-1072, 1961, NASA.

[6] Denison, M. R. and Baum, E., "Compressible Free Shear Layer with Finite Initial Thickness," *AIAA Journal*, Vol. I, No. 2, Feb. 1963, pp. 342–349.

[7] Charwat, A. F. and Der, J., Jr., "Studies on Laminar and Turbulent Free Shear Layers with a Finite Initial Boundary Layer at Separation," CP 4, 1966, AGARD, pp. 215–240.

[8] Chapman, D. R., "A Theoretical Analysis of Heat Transfer in Regions of Separated Flow," TN 3792, 1956, NACA.

[9] Hahn, M., "Experimental Investigation of Separated Flow Over a Cavity at Hypersonic Speed," AIAA Paper 68-672, Los Angeles, 1968.

[10] Smith, A. G. and Spalding, D. B., "Heat Transfer in a Laminar Boundary Layer with Constant Fluid Properties and Constant Wall Temperature," *Journal of the Royal Aeronautical Society*, Vol. 62, Jan. 1958, pp. 60–64.

[11] Kays, W. M., *Convective Heat and Mass Transfer*, 1st ed., McGraw-Hill, New York, 1966, pp. 223–226.

[12] Schlichting, H., *Boundary-Layer Theory*, 6th ed., McGraw-Hill, New York, 1968, p. 322.

Transient Nonlinear Deflections of a Cantilever Beam of Uniformly Varying Length by Numerical Methods

ARMAND L. DILPARE*

Lundy Electronics & Systems, Inc., Glen Head, N.Y.

Introduction

THE exoatomospheric deployment of a long slender radio antenna from an accelerating space vehicle may be dynamically idealized as a cantilever beam of uniformly varying length in a constant gravity field (Fig. 1). The dynamics problem consists in determining, at any instant of time, the relative position and velocity vectors of every point along the beam, i.e., the instantaneous deflection and velocity distribution curves. Qualitatively, if the beam is fairly stiff, and deployment is slow, then the transient deflection curve will be close to the static deflection curve associated with the unsupported length at that instant. Conversely, if the beam is very flexible and/or deployment is rapid, the deflection of the free end will approach the $\frac{1}{2}gt^2$ value.

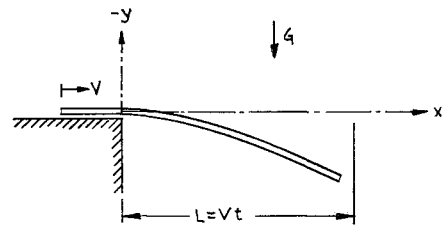

Fig. 1 Antenna deployment geometry.

A numerical method of solution is applied to this problem because deflections and slopes are expected to be large, well into the nonlinear region; and the antenna is nonuniform with a discontinuous distribution of mass and stiffness. The continuous beam structure is replaced with an equivalent lumped-parameter system of elastically coupled rigid bars.[1–4] The accuracy of the approximation improves with an increasing number of bars in the equivalent system. For the present, an equivalent system of six bars has been selected as a compromise between accuracy and computational time.

Equations of Motion for Equivalent System

As shown in Fig. 2, $R_1, R_2, \ldots, R_6$ are the lengths of the beam segments selected so that each segment has uniform properties, i.e., up to five discontinuities may be accommodated. Each segment is replaced with an elastic hinge at its center connecting rigid bars leading to the adjoining segments. The hinge spring constants (K_j) correspond to the rotational deflection of an individual segment under uniform bending moment, i.e.,

$$K_j = E_j I_j / R_j$$

The rigid bars ($S_1, S_2, \ldots, S_6$) have lengths calculated

$$S_1 = \tfrac{1}{2}R_1$$

$$S_j = \tfrac{1}{2}(R_j + R_{j-1}); \quad j > 2$$

and the corresponding masses

$$m_j = \tfrac{1}{2}(\text{mass of } R_j + \text{mass of } R_{j-1}); \quad j > 2$$

The equations of motion are obtained from Lagrange's equations for the six degree-of-freedom system where θ_j = inclination of the jth bar with the coordinate axes (Fig. 2).

The system of equations may be written as

$$A_{ij}\ddot{\theta}_j = B_i; \quad i, j = 1, 2, \ldots 6$$

where the A_{ij} coefficients and B_i terms are functions of $\dot{\theta}_n$,

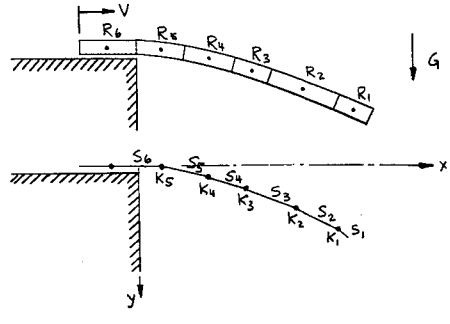

Fig. 2 Equivalent six-bar system.

Received May 11, 1970.

* Associate Director, Research and Development. Member AIAA.

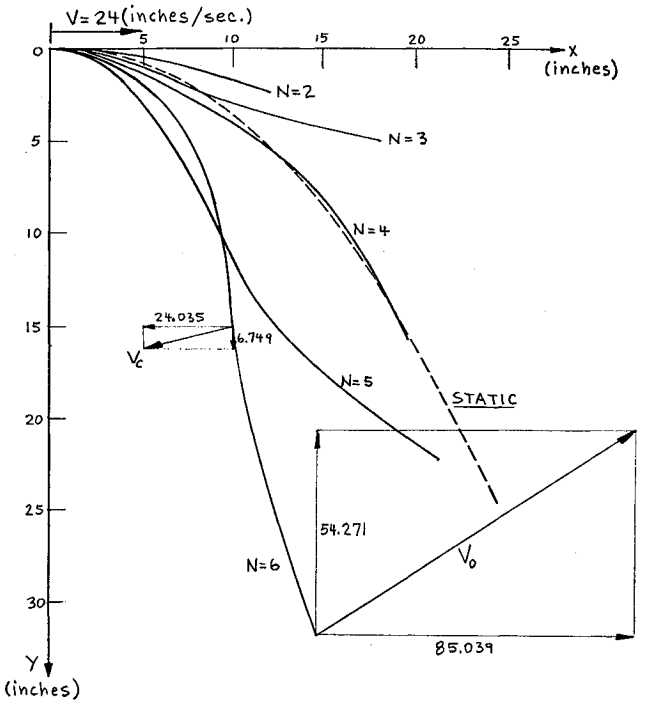

Fig. 3 Instantaneous deflection curves (G = 154.56 in./sec²)

θ_n, R_n, S_n, m_n, G, etc. The expressions are as follows:

$$A_{ij} = \begin{cases} S_j\left(m_j + 2\sum_{\rho=1}^{j-1} m\rho\right)\frac{1}{m_i}\cos(\theta_j - \theta_i); & i > j \\ S_j\left(\frac{2}{3} + \frac{2}{m_j}\sum_{\rho=1}^{j-1} m\rho\right) & i = j \\ S_j\left(1 + \frac{2}{m_i}\sum_{\rho=1}^{i-1} m\rho\right)\cos(\theta_j - \theta_i); & i < j \end{cases}$$

$$B_i = (1/S_i m_i)[k_{i-1}\theta_{i-1} - (k_{i-1} + k_i)\theta_i + k_i\theta_{i+1}] + \cos\theta_i\left[\left(1 + \frac{2}{m_i}\sum_{\rho=1}^{i-1} m\rho\right)G + \sum_{\rho=1}^{i}\dot{\theta}\rho^2\frac{A_i\rho}{S\rho}\sin\theta_j\right] - \sin\theta_i\sum_{\rho=1}^{i}\dot{\theta}\rho^2\frac{A_i\rho}{S\rho}\cos\theta\rho$$

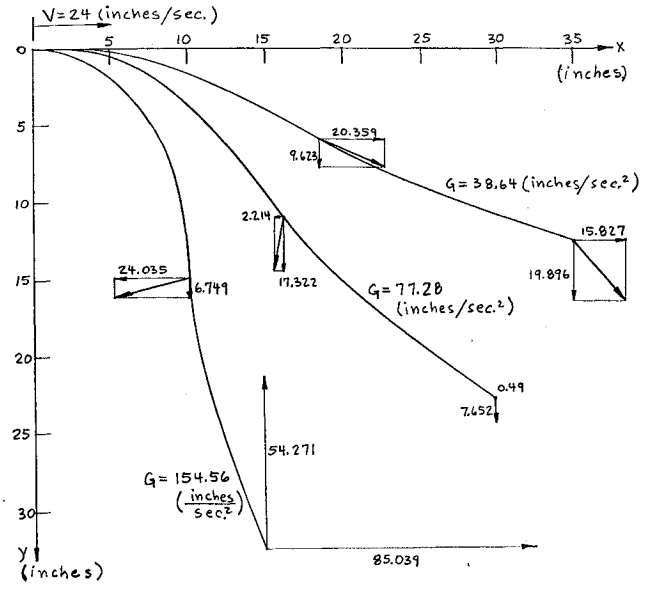

Fig. 4 Instantaneous deflection curves (N = 6).

Solution of the A_{ij} system of equations yields the $\ddot{\theta}_n$ at any instant of time as determined by the system configuration (θ_n and $\dot{\theta}_n$) at that time.

The equations of motion are integrated using an iterative method that calculates $\dot{\theta}_n(t + \Delta t)$ and $\theta_n(t + \Delta t)$ by making use of linear extrapolation over small time increments; more sophisticated methods depending on parabolic or higher order extrapolation were found to be unnecessary.

Now, it is also necessary to replace the uniform motion of the beam with an equivalent discontinuous motion of the six-bar system. The velocity V associates time intervals $T_1, T_2, \ldots, T_6$ with segments $R_1, R_2, \ldots, R_6$ where $T_n = R_n/V$. Starting at $t = 0$ with the free end of R_1 over the support ($x = 0$, $y = 0$), the beam is indexed outboard an amount R_1 and spends a time T_1 in that position. With only one bar active (S_1), the iteration procedure solves the 1×1 system of equations

$$A_{ij}\theta_j = B_i; \quad i, j = 1$$

For the next interval of time T_2, i.e., from $t = T_1$, to $T_1 + T_2$, the beam is indexed an additional amount R_2. Thus, two bars are active (S_1 and S_2), and the system equations $A_{ij}\theta_j = B_i$; $i, j = 1, 2$ are solved each iteration cycle. The procedure continues until the entire beam is cantilevered and the complete system of 6×6 equations are solved each iteration.

Numerical Example

A preliminary design case considers a 38.4-in. long antenna deployed in 1.6 sec from an accelerating vehicle. The deployment velocity of 24 in./sec is at right angles to the acceleration vector. The antenna is a slender uniform steel rod of rectangular cross section (0.036-in. wide and 0.010-in. thick) with bending along the thinner dimension; thus,

$$EI = 0.0942 \text{ lb in.}^2 \text{ and } w = 1.078 \times 10^{-4} \text{ lb./in.}$$

The analysis objectives were to determine the transient deflections and velocities for a range of vehicle accelerations.

Figure 3 contains graphs of instantaneous beam deflection at various instants of time for vehicle acceleration of 154.56 in./sec². The deflection curves are shown at the instants when integer multiples of one-sixth antenna length are cantilevered, i.e., at $N = 6$, the entire length is cantilevered. In the initial phases of beam motion, the cantilevered length is small, the beam is hence very stiff, and transient deflection is small. Since beam deflection varies with the fourth power of length, deflection increases very rapidly in the latter phases of motion. Comparing the dynamic deflection at $N = 6$ with the superimposed graph of static deflection for the fully-extended beam shows a considerable amount of overshoot immediately before the antenna base is arrested and locked in the fully-extended position. The subsequent nonlinear vibration may be obtained with a simple extension of the present analysis; i.e., apply the required arresting forces at the beam base, and let deployment velocity equal zero for a period of time following $N = 6$. This would resolve questions of maximum overshoot deflection and possibility of impact with vehicle and associated maximum bending stress at the base of the beam.

In Fig. 4 are compared dynamic deflection curves (for $N = 6$) at several values of vehicle acceleration. As expected, deflections and associated velocities decrease with decreasing acceleration, but not proportionately.

References

[1] Archer, J. S., "Consistent Mass Matrix for Distributed Mass Systems," *ASCE Structural Division Journal*, Vol. 89, No. ST4, Aug. 1963, pp. 161–178.

[2] Sevcik, J. K., "System Vibration and Static Analysis," 63-AHGT-57, *ASME Aviation and Space Hydraulic and Gas Turbine Conferences*, March 1963.

[3] Beitch, L., "Vibration Response of General Continuous Structures," 67-VIBR-44, *ASME Vibrations Conference*, March 1967.

[4] Pestel & Leckie, *"Matrix Methods in Elastomechanics,"* McGraw-Hill, New York 1963.

Freejet Terminal Shocks

MICHAEL J. WERLE*
Virginia Polytechnic Institute
Blacksburg, Va.
AND
DAVID G. SHAFFER†
AND
RICHARD T. DRIFTMYER‡
U.S. Naval Ordnance Laboratory
White Oak, Silver Spring, Md.

Introduction

THE problem of interest here is that of expanding a two-dimensional gas jet into a quiescent medium. The jets studied are highly underexpanded at their entrance into this medium and subsequently form a classical freejet plume with its attendant barrel and terminal shock waves. The objective of the present study was to provide a suitable means of predicting the terminal shock's position relative to the jet exit plane for jet nozzle Mach numbers equal to or greater than one. Motivation for such an effort has come principally from the field of jet interaction controls where experimental and theoretical studies have indicated that the terminal shock height is a significant scale length. Hence, a definite need exists for a simple model of the two-dimensional freejet (cf., Ref. 1 for further discussion of this point).

Experimental Apparatus and Results

The test apparatus was a flat plate upon which was mounted two-glass-ported side plates for viewing the two-dimensional freejet. The jet issued from a 6-in. span sonic nozzle, flush mounted in the flat plate surface. This entire assembly was installed in a wind-tunnel test cell which served as a controlled pressure reservoir; the reservoir pressures P_∞ being set at either 2 psia or 5 psia for these tests. Three sonic jet nozzles (nominal throat widths of 0.005, 0.020, and 0.030 in.) were tested for a range of jet stagnation pressures which varied from 0–1200 psia, the jet stagnation temperature being constant at 520°R. The flow rate of the jet supply air was measured independently with a standard ASME orifice plate flow meter.

Experimentally observed values of the centerline jet-plume shock height h_s (nondimensionalized by the effective nozzle-exit throat width b_e) are presented in Fig. 1. Also shown are some recent data from Sheeran and Dosanjh[2] who tested weak jets over a limited range of back pressures. Both sets of data are well represented by the relation§

$$h_s/b_e = P_e/P_b \qquad (1)$$

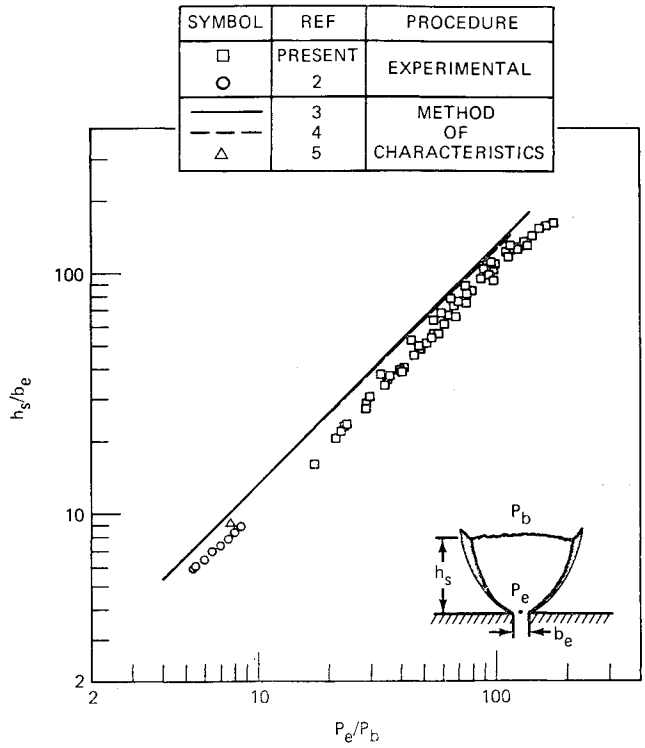

Fig. 1 Two-dimensional freejet terminal shock heights for sonic jets.

To the best of the authors' knowledge, Fig. 1 represents the totality of experimental two-dimensional freejet terminal shock data.

Discussion of Results

One of the principal goals of the present effort was to test the validity of presently available analytical models for the two-dimensional freejet problem. The more sophisticated models employ the method of characteristics to compute the freejet interior flow and thereafter determine the position of the jet shock by either assuming the terminal-shock back pressure, P_b, to be P_∞, or by making some statement about the triple point configuration at the plume termination. The first of these assumptions has more or less stood the test of time for the axisymmetric problem and its application to the two-dimensional problem seems quite natural. Comparison of the solutions so generated by Vinson[3] and Sterret and Barber[4] with experimental results also given in Fig. 1. A second approach, derived from Abdelhamid and Dosanjh,[5] is also given in Fig. 1. The first two solutions differ from the experimental data only by a proportionality constant, and there seems little justification at this point for the added complications advocated in Ref. 5. The exact cause for the observed difference between the theories and the experimental data of Fig. 1 is virtually impossible to isolate among the multitude of possibilities, but there seems little doubt that it is because of differences in detail and not in concept.

Since the two-dimensional experimental data of Fig. 1 was for air expanded through sonic nozzles, the influences of the specific heat ratio γ_e and the jet exit Mach number, M_e, were in question. However, Vinson[3] had used his characteristic solutions to show that there was no appreciable specific heat ratio influence for $1.2 < \gamma_e < 1.4$, but that there was strong dependence on the jet exit Mach number. Although there was no two-dimensional experimental evidence to contradict Vinson's results, it was felt this point needed further study. An attempt was therefore made to use the large reservoir of axisymmetric freejet data to supplement the two-dimensional sonic data. The vehicle for this effort was to be the

Received February 16, 1970; revision received June 25, 1970. The research was sponsored by the Naval Air Systems Command (AIR-320).

* Assistant Professor, Engineering Mechanics Department. Associate Member AIAA.

† Aerospace Engineer, Applied Aerodynamics Division.

‡ Aerospace Engineer, Applied Aerodynamics Division. Member AIAA.

§ The jet-plume back pressure P_b was monitored with a pitot tube placed well above the plume, and in all cases was found to be equal to the reservoir pressure P_∞ to within the accuracy of the instrumentation.